

Supporting Information

Mesoporous Cobalt/ Manganese Oxide: A highly Selective Bifunctional Catalyst for Amine – Imine Transformations

*Biswanath Dutta, Seth March, Laura Achola, Sanjubala Sahoo, Junkai He, Alireza Shirazi Amin, Yang Wu, Shannon Poges, S. Pamir Alpay and Steven L. Suib. **

Content:

Page 3. Chemicals, Preparation of meso-Co-MnO_x, Reaction procedure for amine-alcohol coupling for imine formation.

Page 4. Reaction procedure of diol coupling to form lactone Reaction procedure for reducing imines to secondary amines.

Page 5. Figure S1 (XRD data).

Page 6. Figure S2 (BET-BJH), Figure S3 (SEM-TEM-EDX).

Page 7. Figure S4 (XPS).

Page 8. Figure S5 (ROS studies), Table S1 (XPS data).

Page 9. Table S2 (BET-BJH data), Figure S6 (catalyst loading), Table S3 (solvent screening).

Page 10. Table S4 (optimization of solvent volume), Table S5 (optimization of benzylamine to 4-methoxy benzylalcohol), Table S6 (optimization of reaction environment).

Page 11. Table S7 (Reduction of imines to amines under different reaction conditions), Table S8 (rate constants of various control reactions).

Page 12. Table S9 (Reduction of imines to amines under different high pressure of hydrogen).

Page 13. Table S10 (Di-ol to lactone formation-using different catalysts), Table S11 (Di-ol to lactone formation-using different catalysts).

Page 14. Figure S7 (Leaching test-Hot filtration), Figure S8 (Reusability test and comparison of XRD after fourth cycle).

Page 15. Figure S9 (Time Dependent Study-at different temperatures), Figure S10 (Determination of rate constants- at different temperatures).

Page 16. Figure S11 (K_H/K_D), Figure S12 (Arrhenius plot-Determination of activation energy).

Page 17. Figure S13 (overall reaction mechanism), Figure S14 (H₂-TPR).

Page 18. Computational details, Discussions of Computational Findings.

Page 19-30. NMR spectra.

Chemicals

Manganese (II) nitrate tetrahydrate ($\text{Mn}(\text{NO}_3)_2 \cdot 4\text{H}_2\text{O}$, ≥ 97.0), cobalt (II) nitrate hexahydrate ($\text{Co}(\text{NO}_3)_2 \cdot 6\text{H}_2\text{O}$, ≥ 97.0), 1-butanol (anhydrous, 99.8%), and poly (ethylene glycol)- block-Poly(propylene glycol)-block- Poly (ethylene glycol) PEO₂₀-PPO₇₀-PEO₂₀ (Pluronic P123), Benzylamine, 4-Trifluoromethyl benzylamine, 4-Methoxy benzylamine, 4-Methyl benzylamine, Aniline, 2-Aminomethyl naphthalene, n-Octylamine, n-Butylamine, 4-Nitro benzylamine, 2-Aminomethyl pyrrolidine, 1,2-Benzenedimethanol, 1,3-Benzenedimethanol, 2-Hydroxyphenyl alcohol, 1,2,3,4-Tetrahydroisoquinoline, $\text{C-Mn}_2\text{O}_3$ were purchased from Sigma-Aldrich. Concentrated nitric acid (HNO_3 , 68-70 %) was purchased from J. T. Baker. All chemicals were used as received without further purification.

Preparation of meso-Co-MnOx

The catalyst was synthesized following the procedure described in the literature.^[1] In a typical synthesis 0.02 mol of manganese nitrate tetrahydrate ($\text{Mn}(\text{NO}_3)_2 \cdot 4\text{H}_2\text{O}$), cobalt nitrate hexahydrate ($\text{Co}(\text{NO}_3)_2 \cdot 6\text{H}_2\text{O}$) (depending upon the dopant percentage) and 0.134 mol of 1-butanol were added into a 120 mL beaker. To this solution 0.0034 mol of poly(ethylene glycol)-block-poly(propylene glycol)-block-poly(ethylene glycol) (Pluronic P123, $\text{PEO}_{20}\text{PPO}_{70}\text{PEO}_{20}$, molar mass 5750 g mol^{-1}) and 0.032 mol of concentrated nitric acid (HNO_3) were added and stirred at room temperature until the solution became clear (light pink). The resulting clear solution was then kept in an oven at 120°C for 3 h. The product was collected and washed with excess ethanol, centrifuged, and dried in a vacuum oven overnight. At the end, the dried black powders were subjected to a heating cycle. First, they were heated at 150°C for 12 h and cooled down to room temperature under ambient conditions. The material was then subjected to the following heating cycle to obtain differently calcined materials. 250°C for 3 h, 350°C for 2 h, 450°C for 2 h, 550°C for 1 h and 650°C for 1 h, respectively.

Reaction procedure of amine-alcohol coupling to form imine

In a typical reaction, benzylamine (0.5 mmol), 4-methoxy benzylalcohol (1.2 eqv), catalyst (25 mg) and toluene (1 mL) were added successively in a 25 mL round bottom flask equipped with a condenser.

The reaction mixture was heated to reflux under vigorous stirring (700 rpm) for the required time under an air balloon. After reaction, the reaction mixture was cooled and the catalyst was removed by filtration. The product analysis was done using GC-MS (gas chromatography mass spectrometry). The conversion was determined based on the concentration of benzylamine. Most reactions were repeated twice and the average values were used. The products were isolated by silica gel column chromatography (5:95 Ethyl acetate/petroleum ether was used as an eluent).

Reaction procedure of diol coupling to form lactone

In a typical reaction, 1,2-dimethanolbenzene (0.5 mmol), catalyst (25 mg) and n-butanol (2 mL) were added successively in a 25 mL round bottom flask equipped with a condenser.

The reaction mixture was heated to reflux under vigorous stirring (700 rpm) for the required time under an air balloon. After reaction, the reaction mixture was cooled and the catalyst was removed by filtration. The product analysis was done using GC-MS (gas chromatography mass spectrometry). The conversion was determined based on the concentration of benzylamine. Most reactions were repeated twice and the average values were used. The products were isolated by silica gel column chromatography (5:95 Ethyl acetate/petroleum ether was used as an eluent).

Reaction procedure for reducing imines to secondary amines

In a typical reaction, benzylidene-phenyl-amine (0.5 mmol), catalyst (25 mg) and ethanol: toluene (2 mL) were added successively in a high-pressure reactor.

The reaction mixture was heated to 110 °C under vigorous stirring (700 rpm) for the required time under high pressure of hydrogen. After reaction, the reaction mixture was cooled and the catalyst was removed by filtration. The product analysis was done using GC-MS (gas chromatography mass spectrometry). The conversion was determined based on the concentration of benzylamine. Most reactions were repeated twice and the average values were used. The products were isolated by silica gel column chromatography (5:95 Ethyl acetate/petroleum ether was used as an eluent).

Catalyst Characterization

The powder X-Ray diffraction (PXRD) data were collected by a Rigaku Ultima IV diffractometer (Cu K α radiation, $\lambda=1.5406 \text{ \AA}$) with an operating voltage of 40 kV and a current of 44 mA. The PXRD patterns were collected over a 2θ range of 5–75° with a continuous scan rate of 1.0° min⁻¹. The Nitrogen adsorption desorption experiments were performed with a Quantachrome Autosorb-1-1C automated adsorption system. The samples were treated at 150°C for 6 h under helium prior to measurement. X-ray photoelectron spectroscopy (XPS) was done on a PHI model 590 spectrometer with multiprobes (Φ Physical Electronics Industries Inc.), using Al-K radiation ($\lambda= 1486.6 \text{ eV}$) as the radiation source and was fitted using CasaXPS software (version 2.3.12). The powder samples were pressed on carbon tape mounted on adhesive copper tape stuck to a sample stage placed in the analysis chamber. For correction of surface charging, the C 1s photoelectron line at 284.6 eV was taken as a reference. A mixture of Gaussian (70%) and Lorentzian (30%) functions was used for the least-squares curve fitting procedure. Temperature-programmed reduction (H₂-TPR) analyses were conducted in a programmable tube furnace equipped with a gas analyzer MKS coupled with a quadruple mass selective detector. About 100 mg of materials were packed in a quartz tube reactor mounted into the tube furnace 5 % H₂/ Ar flow was passed through the catalyst bed at a flow rate of 50 sccm, while the temperature was ramped from room temperature (RT) to 800 °C.

a)

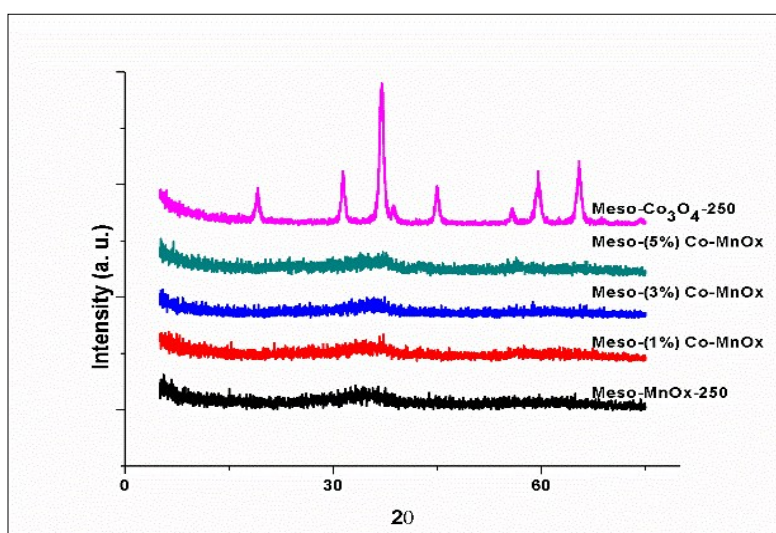


Figure S1. Powder X-ray diffraction of a) meso-MnOx with different percentages of Co, mesoporous CoOx and Meso-MnOx after 250 °C calcination. b) meso-5%Co-MnOx at 250 °C, 350 °C and 450°C calcinations.

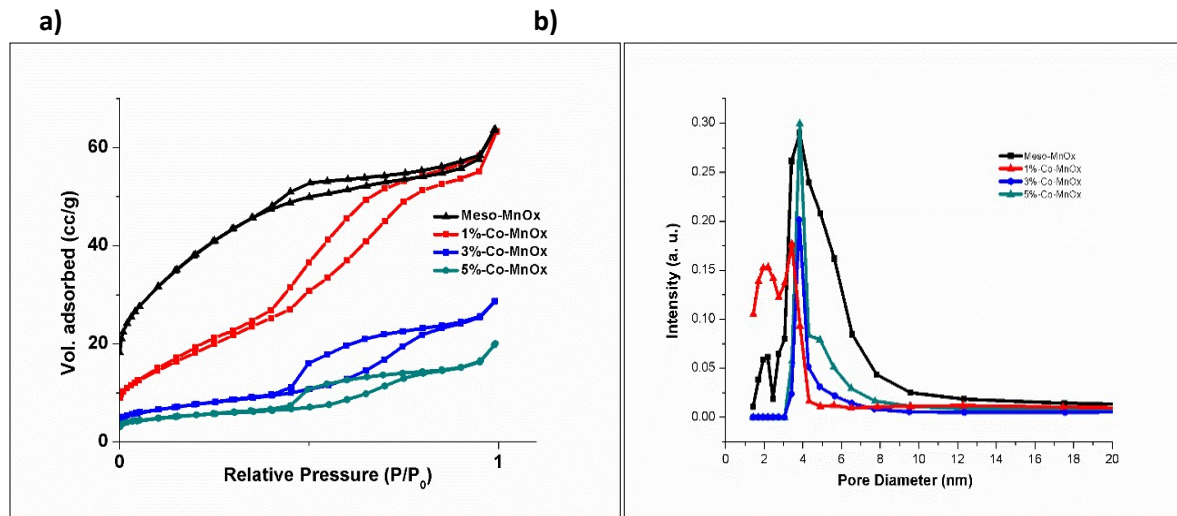


Figure S2. a) Nitrogen adsorption isotherms of meso MnOx with different percentages of Cobalt. A type IV adsorption isotherm followed by a type I hysteresis loop were observed for all the materials, which confirmed the mesoporous structure. b) BJH pore size distribution of the same materials show a constant increase in pore diameter with increasing doping amount.

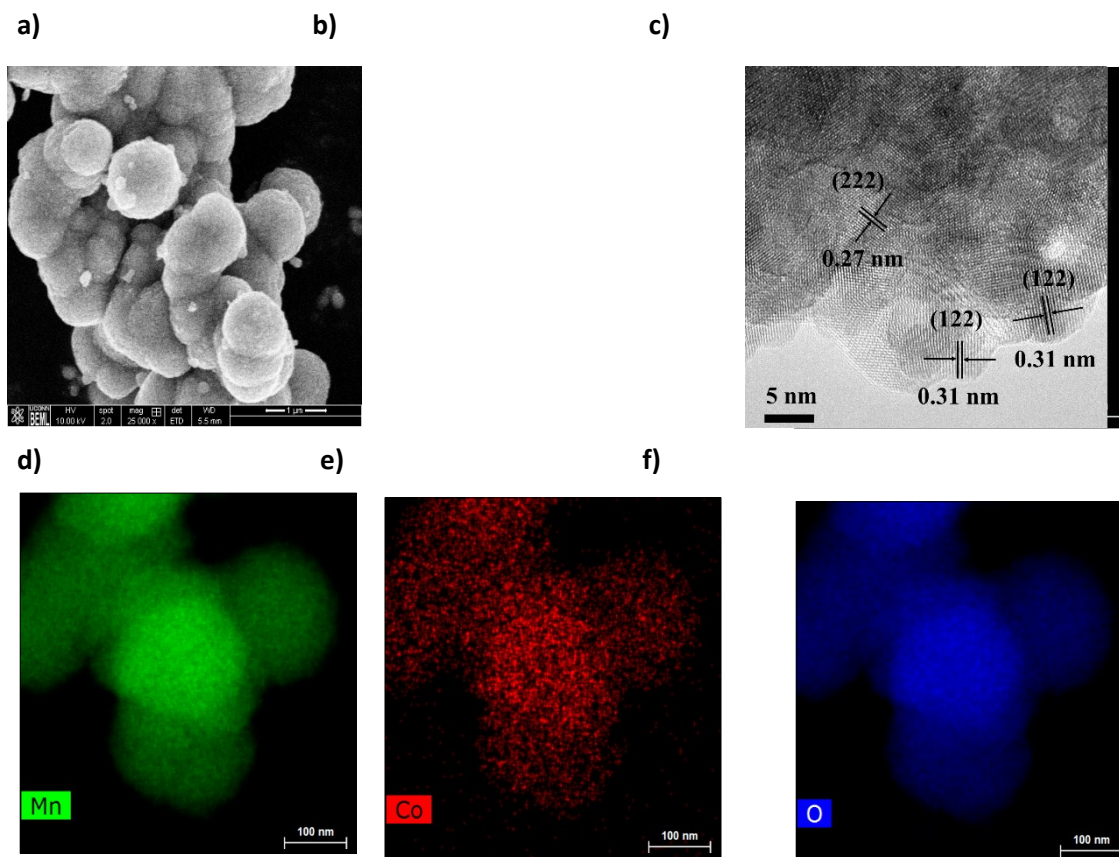
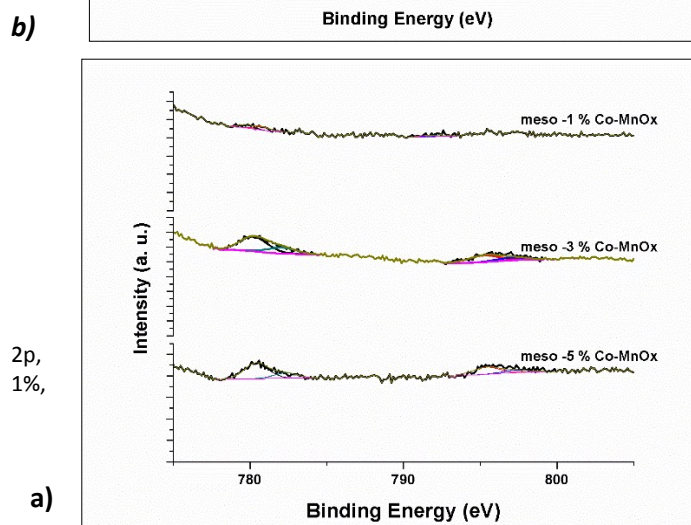
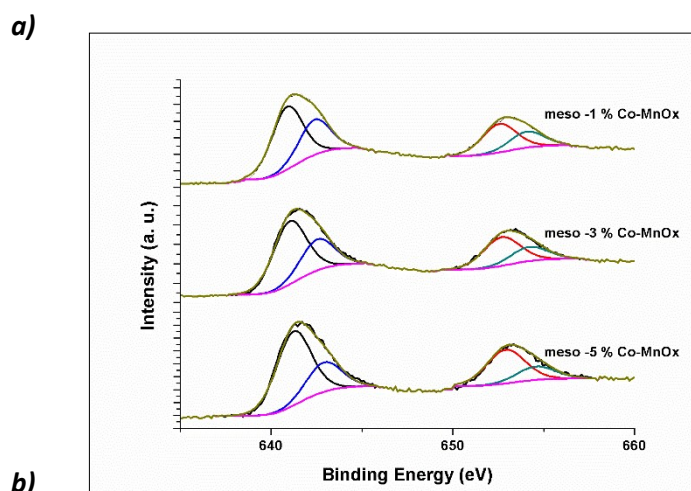


Figure S3. a) SEM, b) HR-TEM, c) HAADF-TEM-EDX, d) mapping of Mn in TEM-EDX, e) mapping of cobalt in TEM-EDX, and f) mapping of O in TEM-EDX of meso-1%-Co-MnOx.



2p,
1%

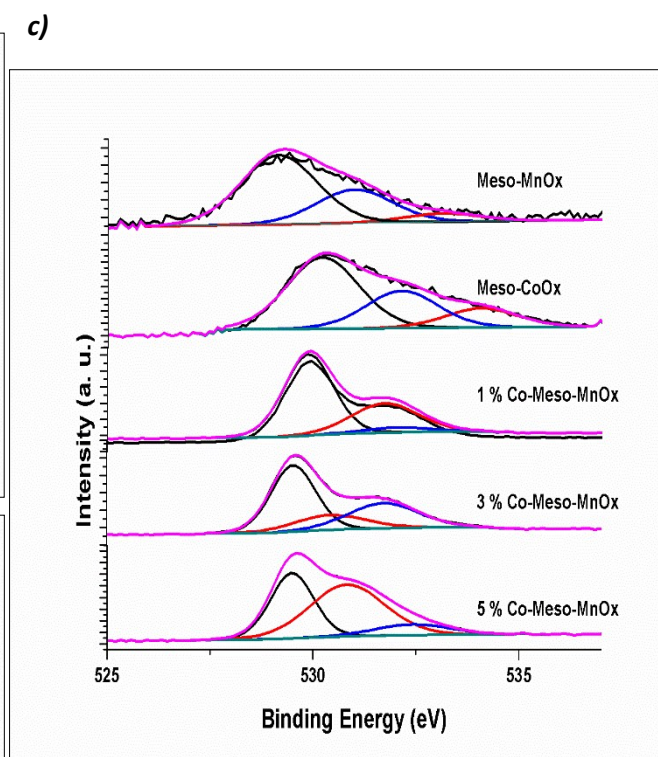
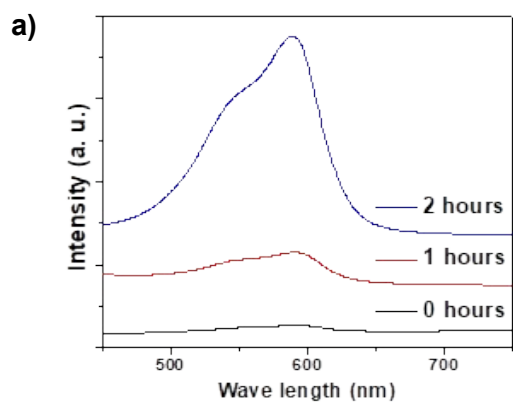
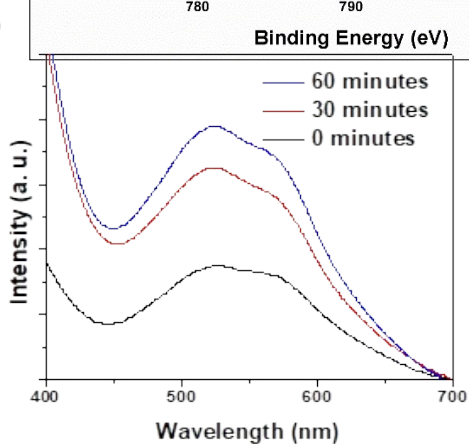
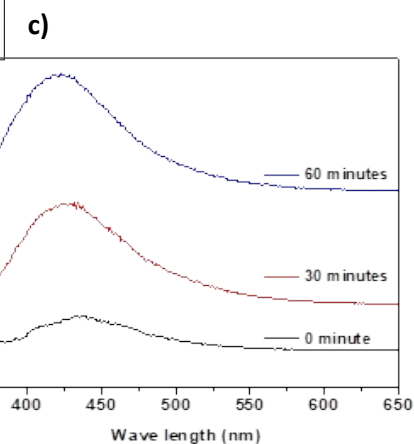


Figure S4. X-ray photoelectron spectra (XPS) of a) Mn b) Co 2P and (c) O 1S of Meso-MnOx, meso-CoOx and 3%, 5% Co doped Meso-MnOx.



d)

Entry	Detected ROS	Additive Used	Quencher Used	Conversion (%) ^a
1.	$O_2^{\cdot-}$	NBT ^b	Curcumin	~15
2.	$\cdot OH$	DST ^c	2,6-Di-tert-butyl-methylphenol (BHT)	0

Figure S5. a) super oxide anion test, b) Peroxide test, and c) hydroxyl radical test. ^a Reaction Conditions: Reaction conditions: benzylamine (0.5 mmol), 4-methoxy benzylalcohol (1.2 eqv.), Toluene (1 mL), 25 mg of catalyst (meso-5%-Co-MnOx), 100°C, 2 hours. ^b NBT = Nitrotetrazolium blue chloride, ^c DST= disodium terephthalate,

Table S1. Summarization of XPS data of meso-MnOx at different calcination temperature.

Entry	Catalyst	Mn ³⁺	Mn ⁴⁺	Co ²⁺	Co ³⁺	O _{lattice}	O _{adsorbed}	O _{adsorbed water}
1	Meso-MnOx	68.25	31.75	N/A	N/A	55.91	29.09	15.00
2	Meso-CoOx	N/A	N/A	28.0	72.0	60.30	30.50	09.20
3	Meso-1% Co-MnOx	64.12	35.88	70.86	29.14	63.54	31.22	05.24
4	Meso-3% Co-MnOx	67.00	33.00	45.05	54.95	51.15	18.11	30.74
5	Meso-5% Co-MnOx	71.60	28.40	75.58	24.42	35.71	53.70	10.59
6.	Meso-MnOx-350	68.83	31.17	N/A	N/A	62.80	25.86	11.30
7.	Meso-MnOx-450	69.63	30.37	N/A	N/A	65.38	23.22	11.40
8.	Meso-5% Co-MnOx-O ₂	71.33	28.67	67.63	32.37	40.19	4.06	55.75
9.	Meso-5% Co-MnOx-N ₂	66.67	33.33	81.13	18.87	11.35	31.33	57.32

Table S2. Structural characterizations of meso MnOx at different calcination temperatures.

Entry	Catalyst	Surface area ^[a] (m ² g ⁻¹)	Pore diameter ^[b] (nm)	Crystal Str. ^[c]
1	Meso-MnOx	100	4.2	Amorphous
2	Meso-1%Co-MnOx	81	3.4	Amorphous
3	Meso-3%Co-MnOx	48	3.8	Amorphous
4	Meso-5%Co-MnOx	34	3.8	Amorphous

^[a] Calculated by BET method. ^[b] Calculated by BJH method from the desorption branch of the isotherm. ^[c] From powder XRD.

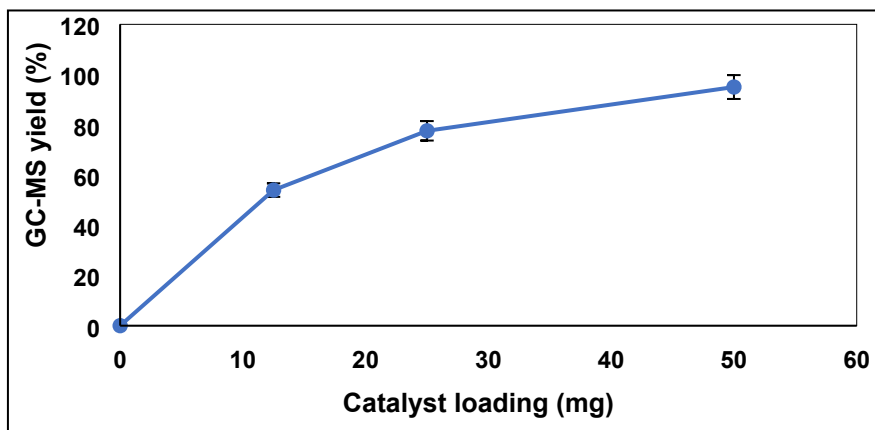


Figure S6. Effect of catalyst loading. Reaction conditions: ^[a] Reaction conditions: benzylamine (0.5 mmol), 4-methoxy benzylalcohol (1.2 eqv.), Toluene (1 mL), 25 mg of catalyst (meso-5%-Co-MnOx), 100°C, 2 hours. ^[b] Conversions and selectivities were determined by GC-MS

Table S3. The catalytic results using different solvents. ^[a]

Entry	Solvent	Relative polarity ²	Conversion (%) ^[b]	Selectivity (%) ^[b]	GC Yield (%) ^[b]	TOF ^[c]
1.	Toluene	0.099	80	97	78	1.26
2.	Benzonitrile	0.333	49	95	47	0.77
3.	Acetonitrile	0.460	12	91	11	0.19
4.	Ethanol	0.654	6	78	5	0.09

^[a] Reaction conditions: benzylamine (0.5 mmol), 4-methoxy benzylalcohol (1.2 eqv.), Toluene (1 mL), 25 mg of catalyst (meso-5%-Co-MnOx), 100°C, 2 hours. ^[b] Conversions and selectivities were determined by GC-MS. ^[c] TOF = TON/ Time (h), TON = no of moles of limiting reagent converted to product per mole of catalyst.

Table S4. The catalytic results using different solvent volumes. ^[a]

Entry	Toluene (mL)	Concentration [g/ L]	Conversion (%) ^[b]	Selectivity (%) ^[b]	Yield (%) ^[b]	TOF ^[c]
1	1	25	80	97	78	1.26
2	2	12.5	74	97	72	1.17
3	5	5	71	90	64	1.12
4	10	2.5	58	83	48	0.91

^[a] Reaction conditions: benzylamine (0.5 mmol), 4-methoxy benzylalcohol (1.2 eqv.), Toluene, 25 mg of catalyst (meso-5%-Co-MnOx), 100°C, 2 hours. ^[b] Conversions and selectivities were determined by GC-MS. ^[c] TOF = TON/ Time (h), TON = no of moles of limiting reagent converted to product per mole of catalyst.

Table S5. The catalytic results using different **benzylamine to 4-methoxy-benzylalcohol** ratio.^[a]

Entry	Bn. amine to 4-OMe-Bn. alcohol ratio	Conversion (%) ^[b]	Selectivity (%) ^[b]	Yield (%) ^[b]	TOF ^[c]
1	1:0.5	48	> 61	29	0.75
2	1:1	69	83	68	1.08
3	1:1.2	80	97	78	1.26
4	0.5:1	82	> 99	81	1.29

^[a] Reaction conditions: benzylamine (0.5 mmol), 4-methoxy benzylalcohol (X eqv.), Toluene (1 mL), 25 mg of catalyst (meso-5%-Co-MnOx), 100°C, 2 hours. ^[b] Conversions and selectivities were determined by GC-MS. ^[c] TOF = TON/ Time (h), TON = no of moles of limiting reagent converted to product per mole of catalyst.

Table S6. The catalytic results using different **oxidants**.^[a]

Entry	Oxidant	Conversion (%) ^[b]	Selectivity (%) ^[b]	GC Yield (%) ^[b]	TOF ^[c]
1	Air	80	97	78	1.26
2	N ₂	66	96	63	1.04
3	O ₂	> 99	> 99	98	1.56

^[a] Reaction conditions: benzylamine (0.5 mmol), 4-methoxy benzylalcohol (1.2 eqv.), Toluene (1 mL), 25 mg of catalyst (meso-5%-Co-MnOx), 100°C, 2 hours. ^[b] Conversions and selectivities were determined by GC-MS. ^[c] TOF = TON/ Time (h), TON = no of moles of limiting reagent converted to product per mole of catalyst.

Table S7. Reduction of imines to amines under different **reaction conditions**.^[a]

Entry	Catalyst	Conversion (%) ^[b]	Selectivity (%) ^[b]			GC Yield (%) ^[b]	TOF ^[c]
			aldehyde	aniline	amine		
1. ^d	Meso-5%-Co-MnOx	84	2.5	2.5	95	80	0.88
2. ^d	Meso-5%-Co-MnOx (reduced)	37	N/A	N/A	> 99	37	0.39

3. ^d	Meso-10%-Co-MnOx	60	N/A	N/A	> 99	59	0.63
4. ^e	Meso-5%-Co-MnOx	> 99	48 ^f	48	4	4	1.04
5. ^d	Meso-1%-Co-MnOx	79	N/A	N/A	> 99	78	0.83
6. ^d	Meso-MnOx	69	N/A	N/A	> 99	68	0.72
7. ^d	Meso-CoOx	58	N/A	N/A	> 99	57	0.61
8. ^d	Catalyst free	68	N/A	N/A	> 99	67	0.71

[a] Reaction conditions: benzylidene phenyl imine (0.5 mmol), Toluene (2 mL), 25 mg of catalyst, 100°C, 3 hours. [b] Conversions and selectivities were determined by GC-MS. [c] TOF = TON/ Time (h), TON= TON = no of moles of limiting reagent converted to product per mole of catalyst. [d] NaBH₄, [e] hydrazine hydrate (N₂H₄.H₂O), and [f] produced aldehyde coupled with the unreacted hydrazine hydrate to form Ph-HC=N-N=CH-Ph.

Table S8. Rate constants of different percentage of different oxidation reactions in presence of meso-MnOx, meso-CoOx and cobalt doped meso-MnOx catalysts.

Catalysts	Benzylamine coupling ($k_1 + k_2 + k_3$) (min ⁻¹)	Benzylalcohol oxidation (k_4) (min ⁻¹)	Benzaldehyde - Benzylamine coupling (k_5) (min ⁻¹)	Benzalalcohol - Benzylamine coupling (min ⁻¹)
Meso-MnOx	0.0199	0.0040	0.0623	0.0177
Meso-CoOx	0.0004	0.0013	0.0657	<i>Not calculated</i>
Meso-1% Co-MnOx	0.0023	0.0053	0.0683	0.0198
Meso-3% Co-MnOx	0.0017	0.0052	0.0651	<i>Not calculated</i>
Meso-5% Co-MnOx	0.0011	0.0050	0.0644	<i>Not calculated</i>

p.s. k_1 , k_2 , k_3 , k_4 and k_5 , refers to the rate constants as shown in reaction mechanism **Scheme 5**.

Table S9. Reduction of imines to amines under different **high pressure of hydrogen**. ^[a]

Entry	Catalyst	Conversion (%) ^[b]	Selectivity (%) ^[b]			TOF ^[c]
			aldehyde	aniline	alcohol	
1.	Meso-10%-Co-MnOx	43	50	50	N/A	0.22
2.	Meso-10%-Co-MnOx (reduced)	12	N/A	50	50	0.06

3.	Meso-5%-Co-MnOx	51	50	50	N/A	0.26
4.	Meso-5%-Co-MnOx (reduced)	13	N/A	50	50	0.06
5.	Meso-1%-Co-MnOx	72	50	50	N/A	0.38
6.	Meso-1%-Co-MnOx (reduced)	16	N/A	50	50	0.08
7.	Meso-MnOx	15	50	50	N/A	0.08
8.	Meso-CoOx	12	N/A	50	50	0.06
9. ^d	Meso-1%-Co-MnOx	10	50	50	N/A	0.06
10. ^e	Meso-1%-Co-MnOx	75	50	50	N/A	0.38

[a] Reaction conditions: benzylidene phenyl imine (0.5 mmol), Toluene (2 mL), 25 mg of catalyst, 100°C, 6 hours. [b] Conversions and selectivities were determined by GC-MS. [c] TOF = TON/ Time (h), TON= TON = no of moles of limiting reagent converted to product per mole of catalyst. [d] 200 psi, [e] 400 psi.

Table S10. Di-ol to lactone formation-using different catalysts. ^[a]

Entry	catalyst	Conversion (%) ^[b]	Selectivity (%) ^[b]	GC Yield (%) ^[b]	TON ^[c]
1.	MnOx	25	> 99	25	0.79
2.	CoOX	8	> 99	8	0.25
3.	Meso-1% Co-MnOx	70	> 99	69	2.20

4.	Meso-3% Co-MnOx	45	> 99	45	1.42
5.	Meso-5% Co-MnOx	39	> 99	39	1.23
6.	Meso-5% Mn-CoOx	10	43	4	0.31

^a Reaction conditions: benzene-1,2-dimethanol (0.5 mmol), Toluene (2 mL), 25 mg of catalyst, 100°C, 6 hour. ^b Conversions and selectivities were determined by GC-MS. ^c TON = no of moles of limiting reagent converted to product per mole of catalyst.

Table S11. Di-ol to lactone formation-using different solvents. ^[a]

Entry	catalyst	Solvents	Conversion (%) ^[b]	Selectivity (%) ^[b]	GC Yield (%) ^[b]	TON ^[c]
1.	1%-Co	Acetonitrile	36	8	3	0.05
2.		Benzonitrile	10	> 99	10	0.01
3.		n-Butanol	> 99	> 99	98	0.13
4.		Toluene	70	> 99	69	2.20
5.		1-Octanol	90	80	72	0.12

^a Reaction conditions: benzene-1,2-dimethanol (0.5 mmol), solvent (2 mL), 25 mg of catalyst (Meso-1% Co-MnOx), 100°C, 6 hours.

^b Conversions and selectivities were determined by GC-MS. ^c TON = no of moles of limiting reagent converted to product per mole of catalyst.

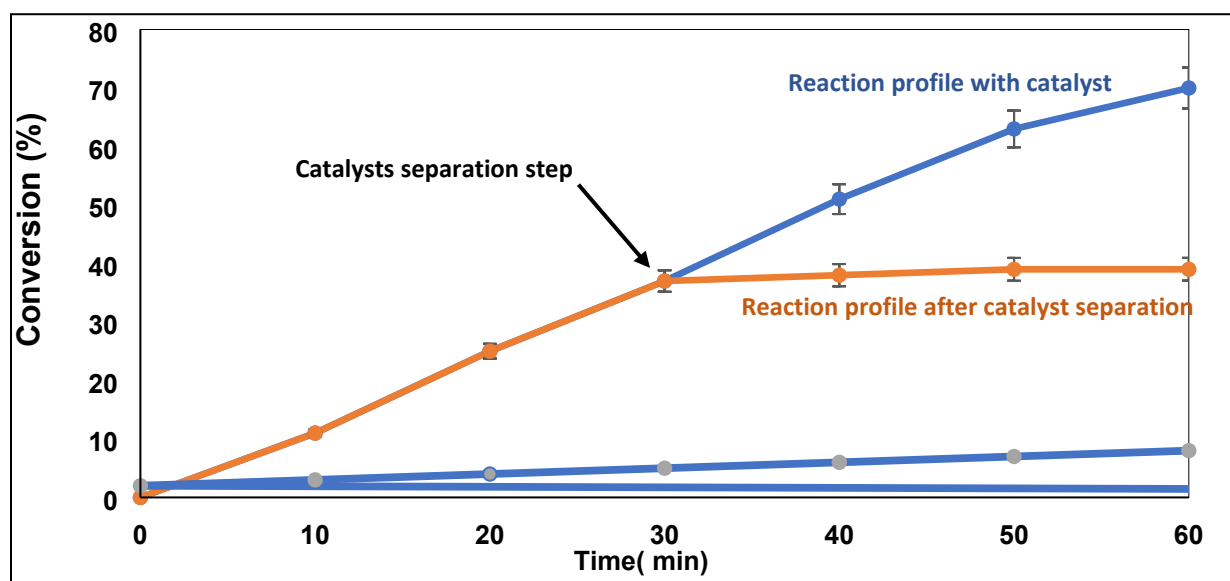


Figure S7. Leaching test of the dehydrogenative coupling of **4-methoxybenzylalcohol** and **benzylamine**: Reaction conditions: benzylamine (0.5 mmol), 4-methoxy benzylalcohol (1.2 eqv.), Toluene (1 mL), 25 mg of catalyst (meso-1% Co-MnOx calcined up to 250 °C), 100 °C. After 3 h, meso-Co-Mn₂O₃ was removed by hot filtration (at about 37 % conversion).

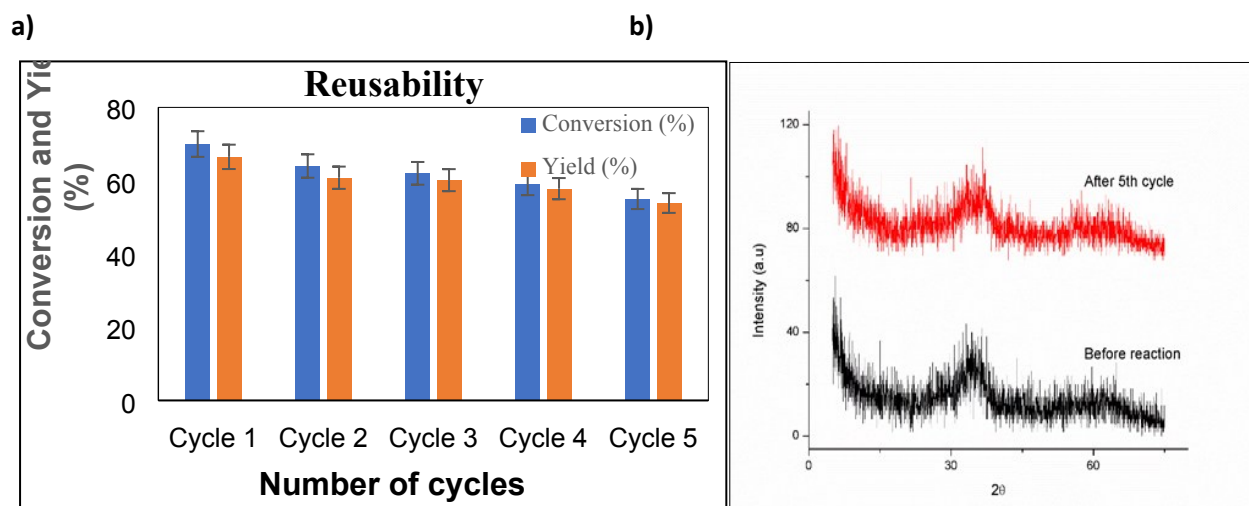


Figure S8. a) Reusability test of the catalyst. Reaction condition: benzylamine (0.5 mmol), 4-methoxy benzylalcohol (1.2 eqv.), Toluene (1 mL), 25 mg of catalyst (meso-5%-Co-MnOx), 100°C, 2 hours. ^{b)} Conversions and selectivities were determined by GC-MS. Turnover number (TON) = [reacted mol benzylamine]/[total mol catalyst]. b) PXRD of meso MnOx-550 before and after fourth reuse. No noticeable changes were observed in the diffraction patterns after fourth reuse.

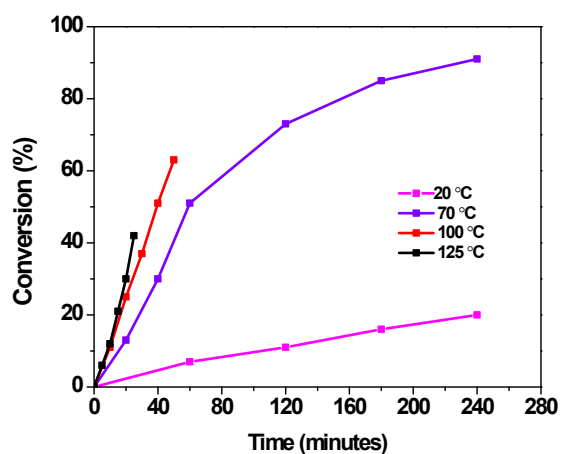


Figure S9. Time Dependent Study. Reaction procedures were the same as discussed in Figure S6.

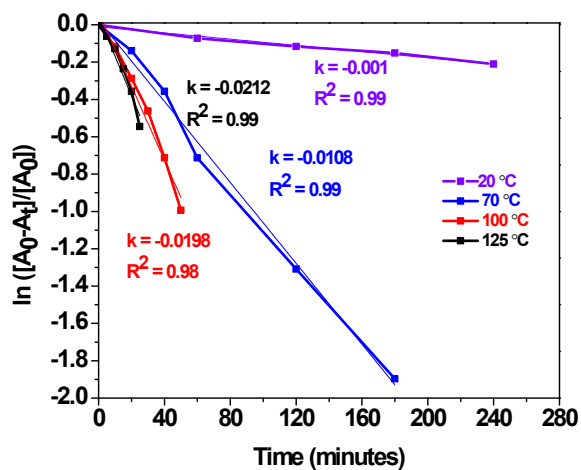


Figure S10. Kinetic study of the cross coupling of *benzylamine* and *benzylalcohol* by meso-1%Co-MnO_x: The reaction exhibited a first order rate dependence with respect to the *benzylamine*, having the rate constant of 0.013 h⁻¹.

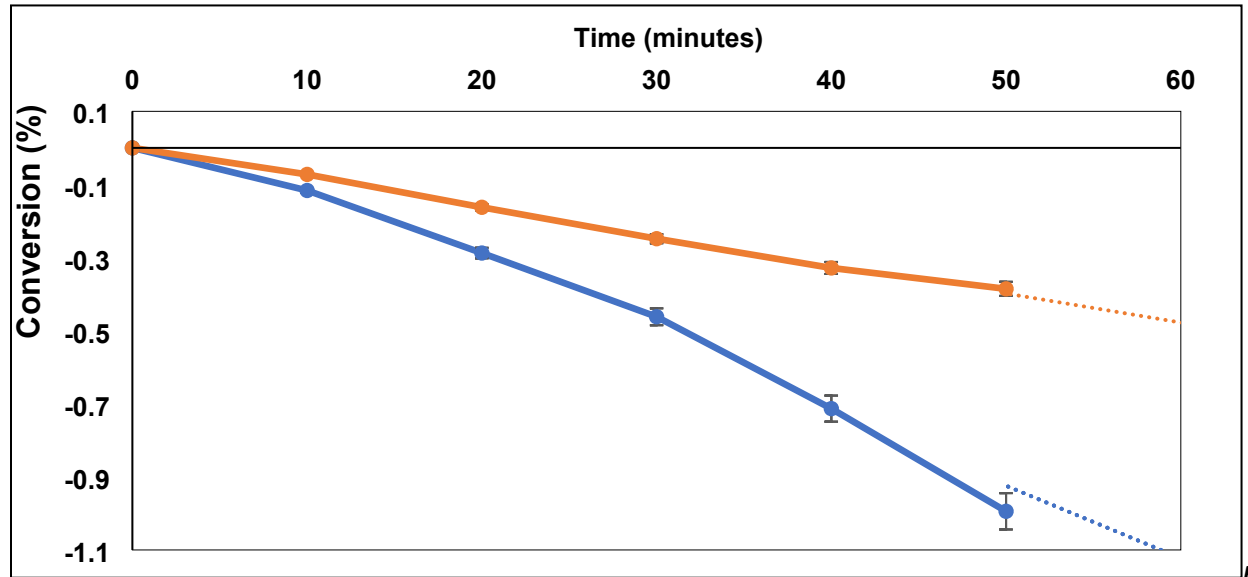


Figure S11. Kinetic study of cross coupling of *benzylamine* and *benzylalcohol* by meso-1%Co-MnO_x: The reaction exhibited a first order rate dependence with respect to the *benzylamine*, having the rate constant of 0.013 h⁻¹.

Reaction conditions: *benzylamine* (0.25 mmol), *benzylalcohol* (1.2 eqv.), toluene (1 mL), 25 mg of catalyst (Meso-1%Co- MnO_x), 100°C.

A₀: original concentration of substrate. A_t: concentration of substrate at time t. K: rate constant.

K_H/K_D for the deprotonation of α -CH₂ of *benzylamine* = 0.0198/ 0.008 = 2.48

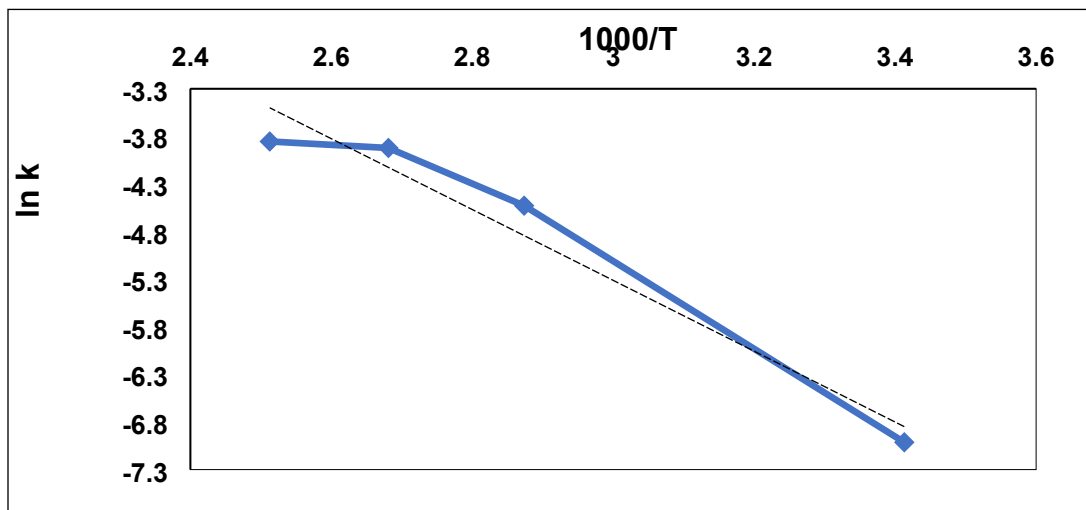


Figure S12. Arrhenius plot for oxidative coupling of benzylamine and benzylalcohol by meso-1%Co-MnO_x: The apparent activation energy was estimated as 30.85 KJmol⁻¹. Reaction conditions: benzylamine (0.25 mmol), benzylalcohol (1.2 eqv.) toluene (1 mL), 25 mg of catalyst (Meso-1%Co- MnOx), 100°C, air balloon. K: rate constant.

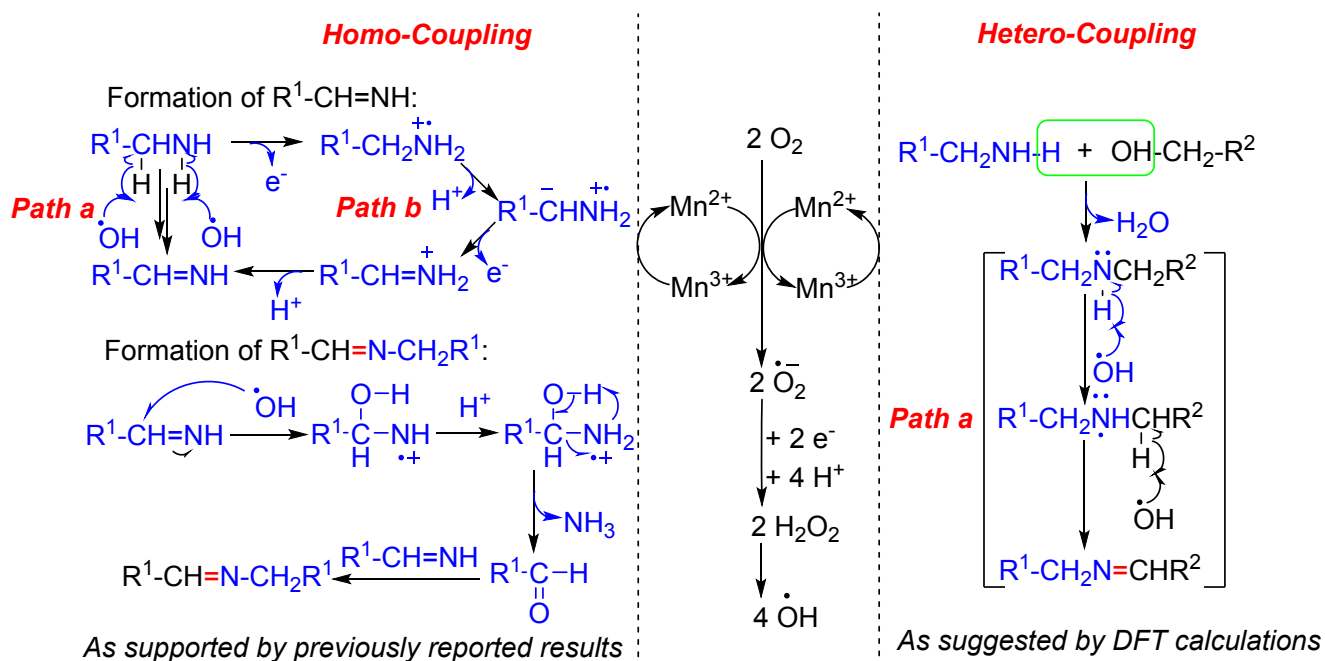


Figure S13. Proposed overall reaction mechanism for imine formation over meso-Co-MnO_x.

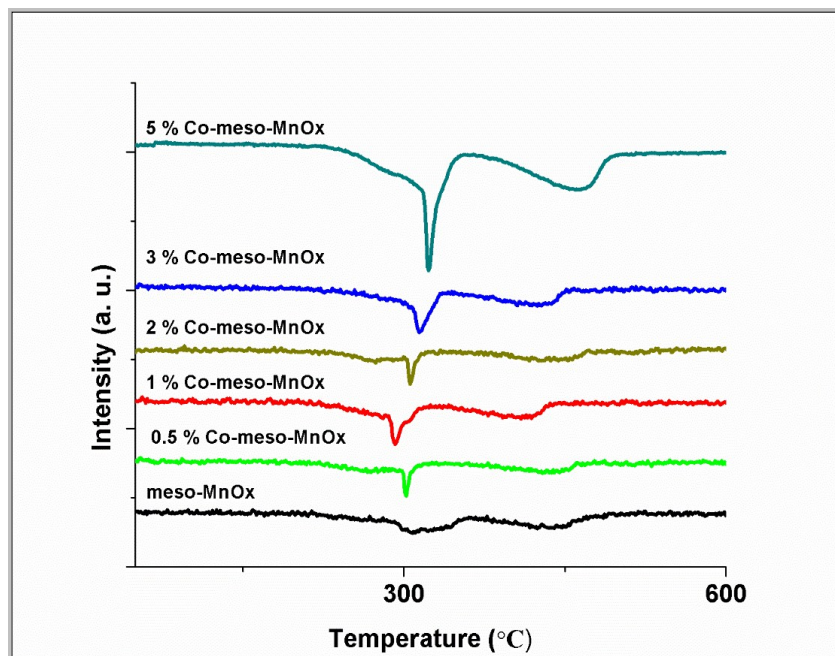


Figure S14. H₂-TPR of different percentage of cobalt doped meso-MnOx.

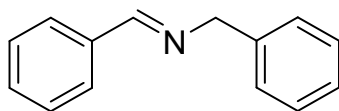
Computational Details

Density functional calculations were carried out to understand the role of Co doping in the enhancement of activity for oxidative dehydrogenative coupling reaction of benzylamine (C₇H₉N) on meso-MnOx (100) surface. Semi-infinite slab models were prepared for meso-MnOx (100) by taking four atomic layers with each layer containing 64 atoms. Two bottom layers are constrained to the bulk positions and the system is geometrically optimized with the vacuum thickness is set to 20 Å. The lateral dimension of the supercell is kept relatively large, $L_x = L_y = 17.99 \text{ \AA}$, in order to deposit the reactant molecules and keeping the periodic interaction between them at its minimum. The Brillouin zone integration was done with $3 \times 3 \times 1$ k-space grid. Plane wave cut-off for the wave functions was set to 400 eV. Spin-polarized calculations were done taking care the magnetic ordering, such that the Mn moments are anti-parallel and the total magnetic moment in each layer lead to zero μ_B . The Vienna ab initio Simulation Package (VASP)^{1,2} was used to perform the calculations. The generalized gradient approximation³ was used along with Hubbard U⁴ correction on the d-orbitals of Mn and Co species with a value of 4 eV.

Discussions of Computational Findings

Our finding shows that the complete reaction could proceed in two main steps. In step I, a water molecule is released when the benzyl amine (C_7H_9N) and benzyl alcohol (C_7H_8O) react on meso-MnOx surface, leading to a reduced intermediate complex [$C_7H_8N-C_7H_7$]. In step II, the intermediate complex [$C_7H_8N-C_7H_7$] loses a H_2 molecule to give the product. The later step was found to be the rate determining step, which we modelled to capture the reaction energetics. The [$C_7H_8NC_7H_7$] intermediate complex was first stabilized on pure meso-MnOx (100) and Co doped meso-MnOx (100) surfaces, where the Co atom is substituted with a Mn site on the surface layer. Energetics of the final step was compared for both pure and Co-doped meso-MnOx surfaces. Our findings show that the intermediate molecule was more stable when it was bonded to the meso-MnOx surface through a nitrogen. In order to determine the activation barrier, the constrained geometry optimization method is adopted where 8 images were generated linearly from the intermediate reactant to the product state. The magnetic moment of the linear images for meso-MnOx (100) was zero, while Co doped meso-MnOx (100) yielded 2 μ_B . The N atom and one of the H atoms of the H_2 molecule are kept fixed to constrain their bond length (defined as the reaction coordinate) and the rest atoms are geometrically optimized. **Figure 2** shows the reaction pathway for meso-MnOx (100) (*black curve*) and Co doped meso-MnOx (100) (*red curve*). It is found that the activation barrier is reduced by 112 meV upon Co doping. This gives a hint that Co changes the electronic structure and assists the chemical reaction by reducing the activation barrier. Such analysis could be easily carried out to identify the role of other surface point defects, such as oxygen-vacancy, which will be carried out in future.

Characterization of typical products

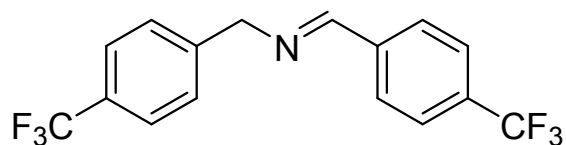


N-benzylidene benzylamine

Appearance: Yellow oil

^1H NMR (400 MHz, Chloroform-*d*): δ 8.32 (t, J = 1.4 Hz, 1H), 7.74 – 7.68 (m, 2H), 7.34 (d, J = 2.2 Hz, 2H), 7.33 (d, J = 1.8 Hz, 1H), 7.27 (s, 2H), 7.26 (s, 2H), 7.21 – 7.16 (m, 1H), 4.75 (d, J = 1.5 Hz, 2H).

^{13}C NMR (101 MHz, Chloroform-*d*): δ 162.10, 139.44, 136.31, 130.88, 128.72, 128.62, 128.40, 128.10, 127.11, 65.18.

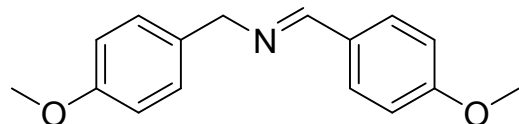


N-(4-(trifluoromethyl)benzylidene)(4-(trifluoromethyl)phenyl)methanamine

Appearance: Yellow oil

^1H NMR (400 MHz, Chloroform-*d*): δ 8.47 (s, 1H), 7.91 (d, J = 7.9 Hz, 2H), 7.69 (d, J = 8.0 Hz, 2H), 7.62 (d, J = 7.9 Hz, 2H), 7.48 (d, J = 7.8 Hz, 2H), 4.90 (s, 2H).

^{13}C NMR (101 MHz, Chloroform-*d*) δ 160.91, 142.85, 138.83, 128.34, 127.94, 125.39 (dd, J = 16.5, 3.6 Hz), 64.22.

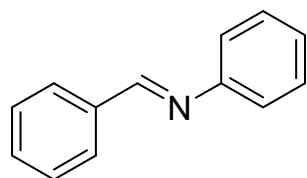


N-(4-methoxybenzylidene)(4-methoxyphenyl)methanamine

Appearance: Yellow oil

^1H NMR (400 MHz, Chloroform-*d*) δ 8.68 (s, 1H), 8.11 (d, J = 8.6 Hz, 2H), 7.64 (d, J = 8.4 Hz, 2H), 7.37 – 7.22 (m, 4H), 5.11 (s, 2H), 4.20 (d, J = 14.6 Hz, 6H).

^{13}C NMR (101 MHz, Chloroform-*d*) δ 162.06, 161.28, 159.04, 132.09, 130.19, 129.55, 114.33 (d, J = 6.7 Hz), 64.79, 55.72.

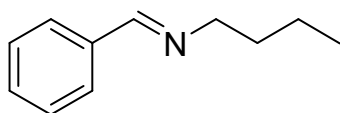


N-benzylidenebenzenamine

Appearance: Yellow oil

^1H NMR (400 MHz, Chloroform-*d*): δ 8.54 (s, 1H), 8.08 – 7.97 (m, 2H), 7.57 (hept, $J = 3.6$ Hz, 3H), 7.50 (t, $J = 7.8$ Hz, 2H), 7.37 – 7.32 (m, 3H).

^{13}C NMR (101 MHz, Chloroform-*d*) δ 160.02, 151.76, 135.92, 131.04, 128.85, 128.51, 128.44, 125.64, 120.59.



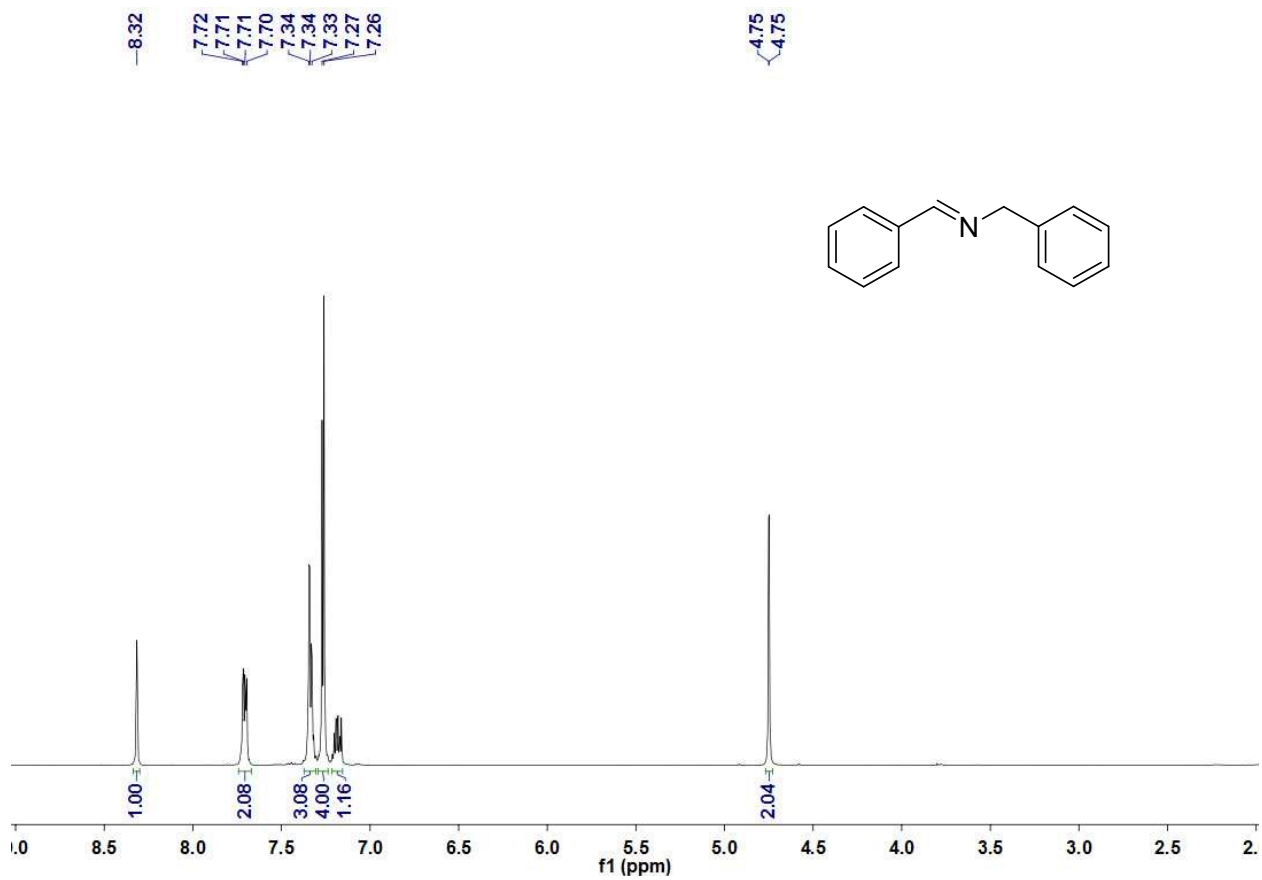
N-benzylidenebutan-1-amine

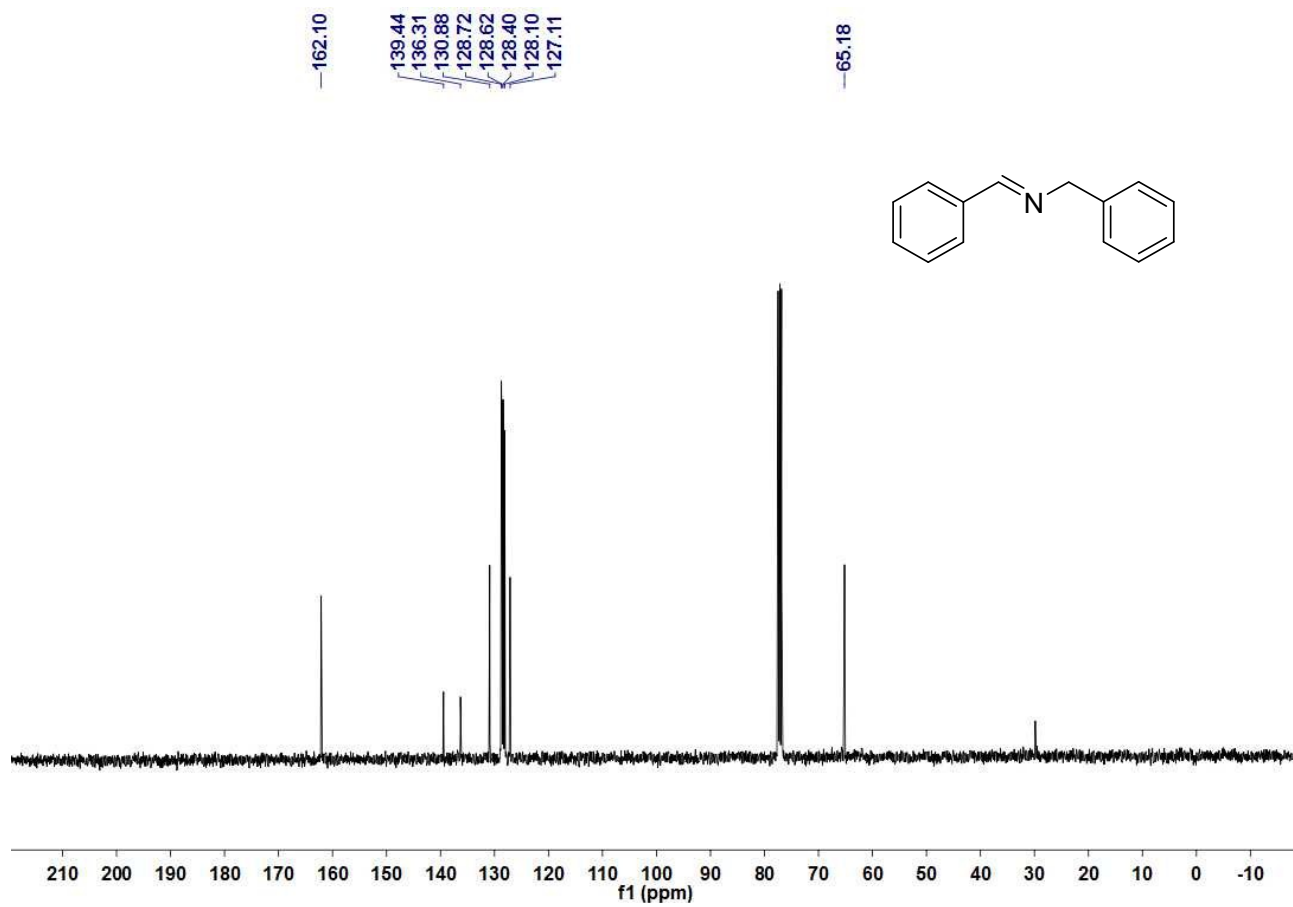
Appearance: colourless oil

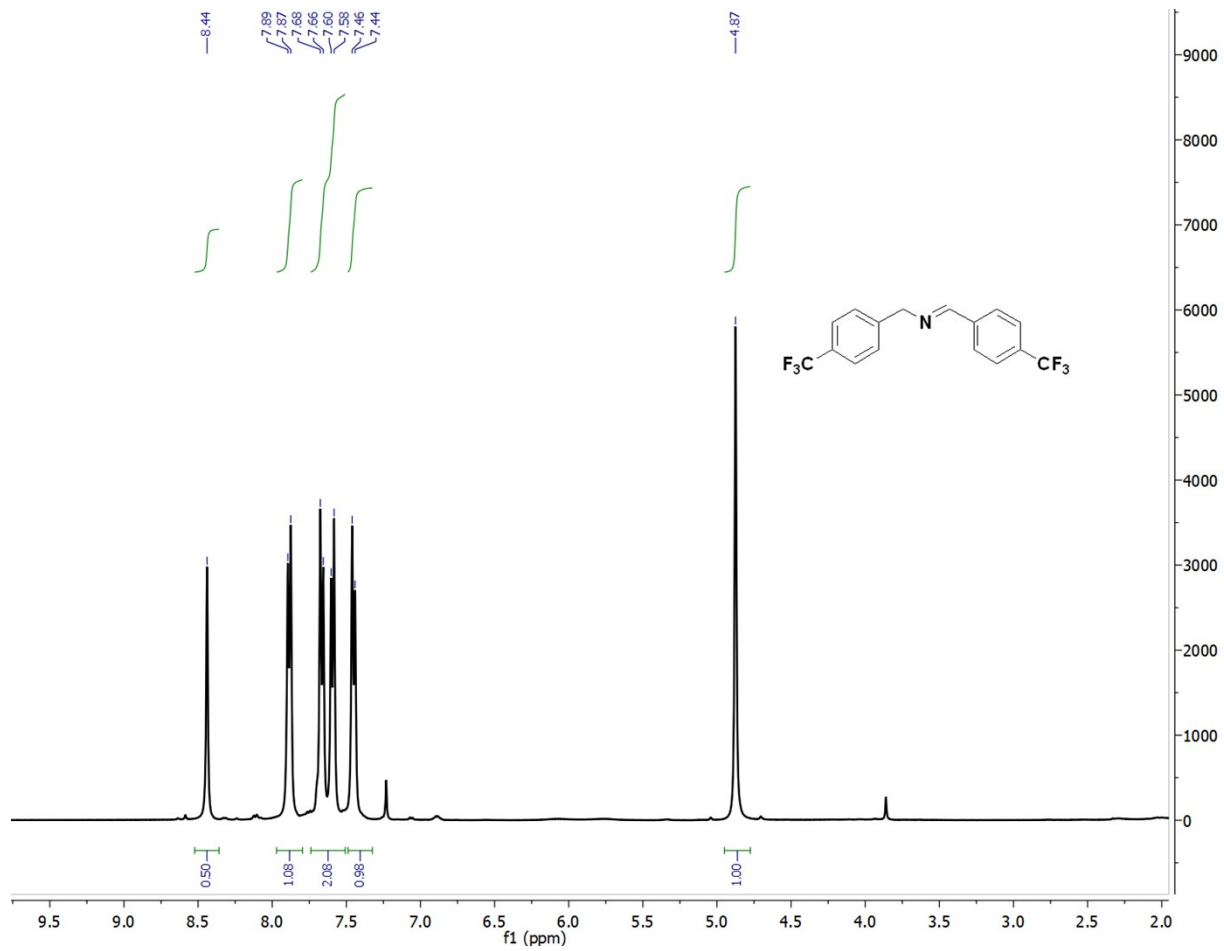
^1H NMR (400 MHz, Chloroform-*d*): δ 8.13 (t, $J = 1.3$ Hz, 1H), 7.66 – 7.54 (m, 2H), 7.31 – 7.23 (m, 3H), 3.48 (td, $J = 7.0, 1.4$ Hz, 2H), 1.66 – 1.49 (m, 1H), 1.30 – 1.20 (m, 2H), 0.82 (t, $J = 7.4$ Hz, 3H).

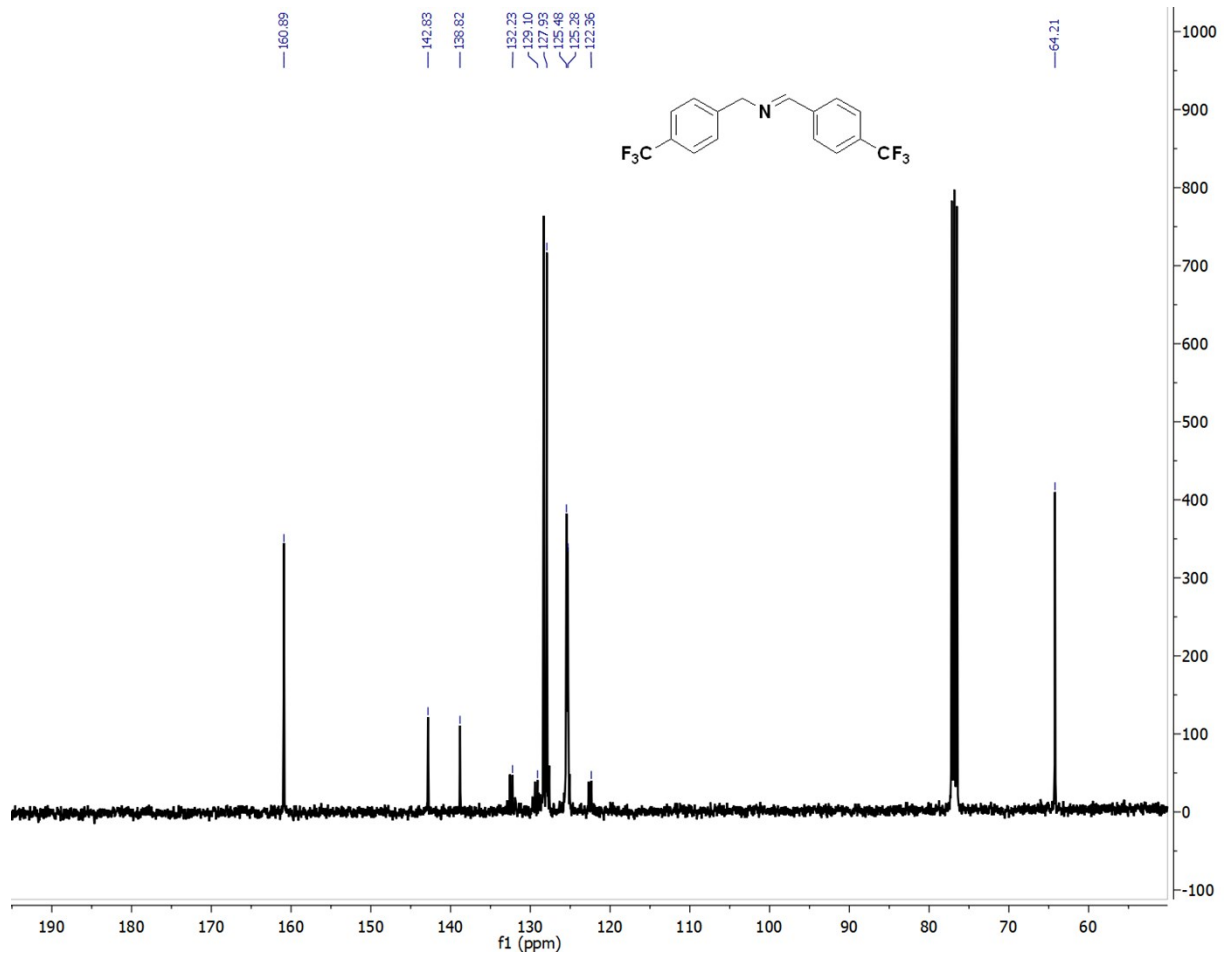
^{13}C NMR (101 MHz, Chloroform-*d*): δ 160.79, 136.45, 130.49, 128.62, 128.09, 61.53, 33.09, 20.54, 13.98.

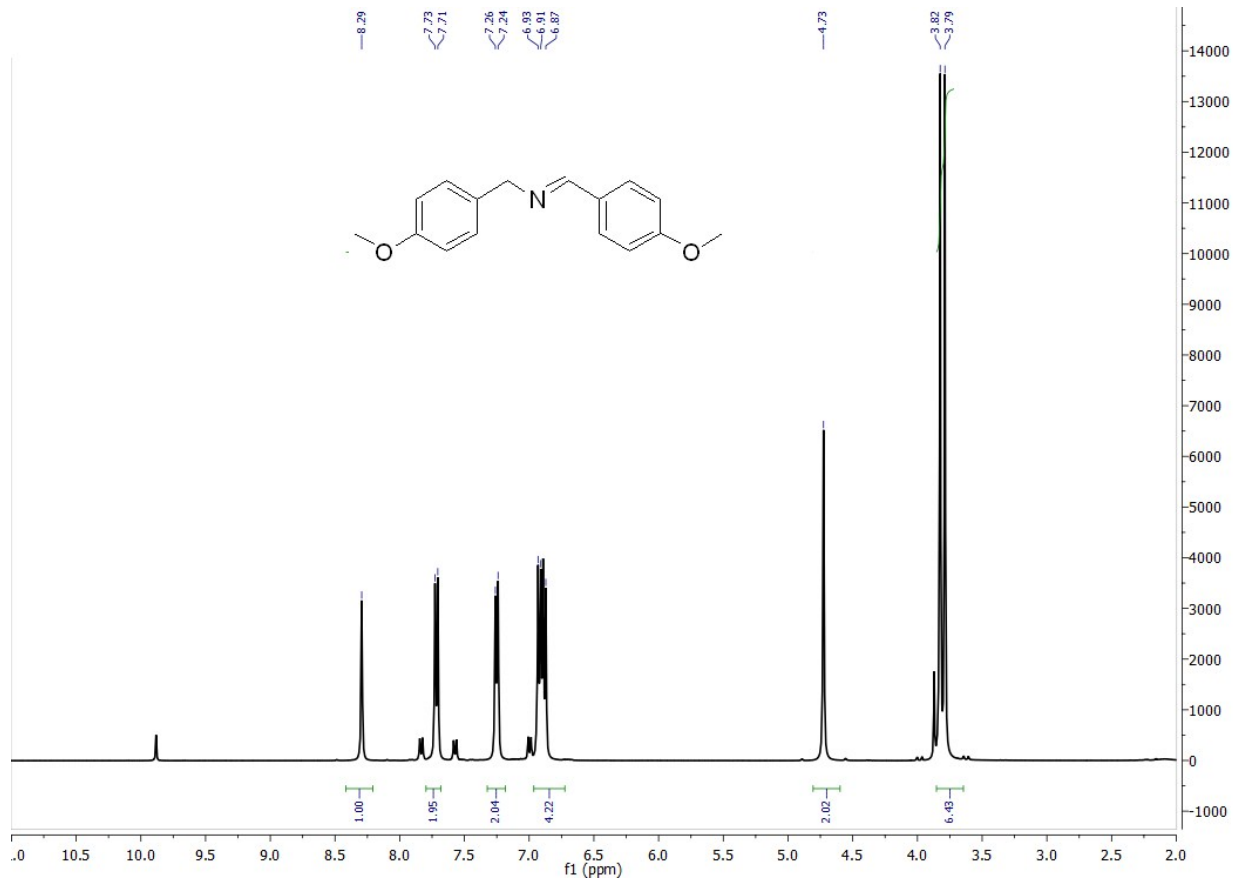
^1H NMR and ^{13}C NMR of typical products

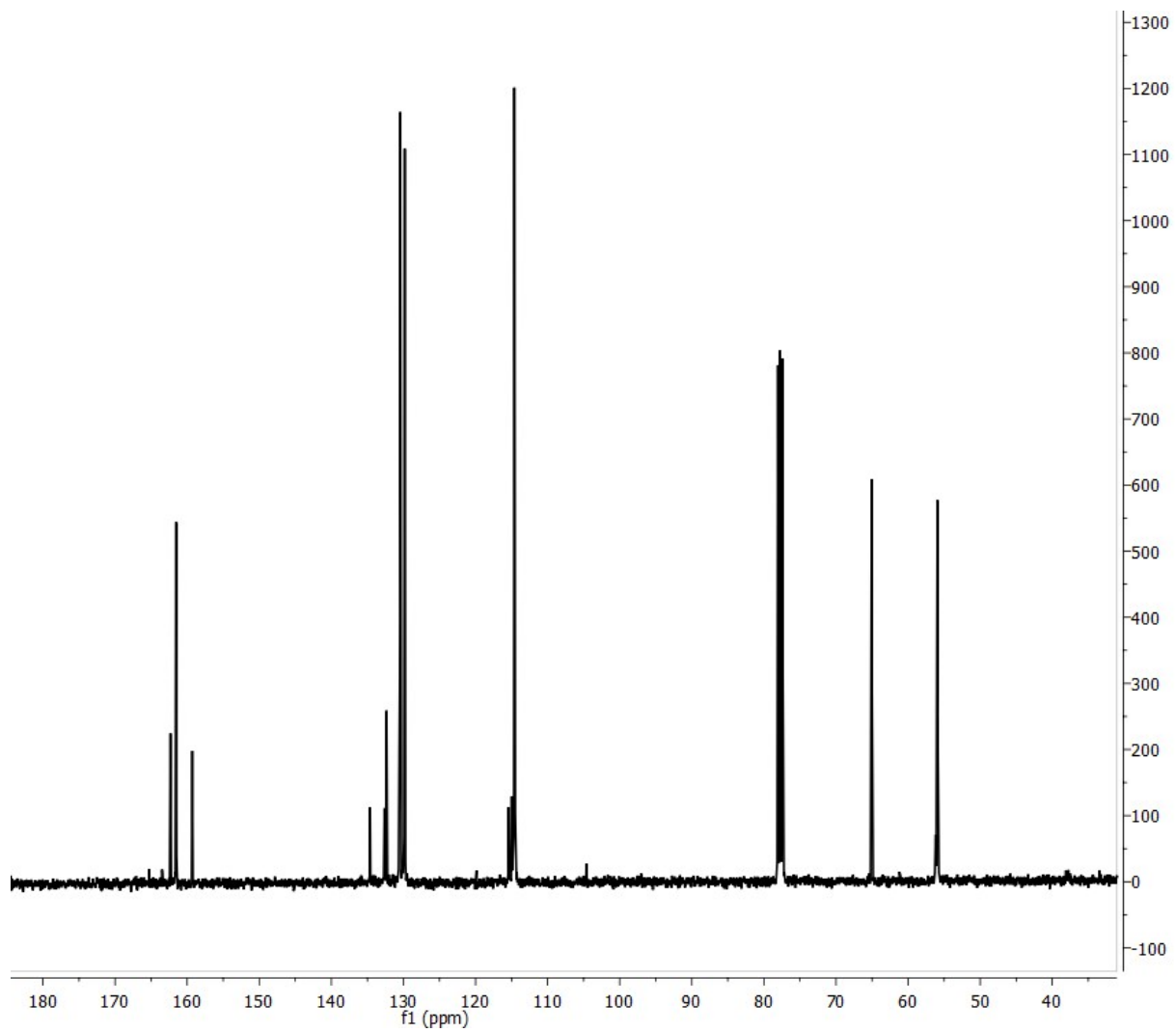


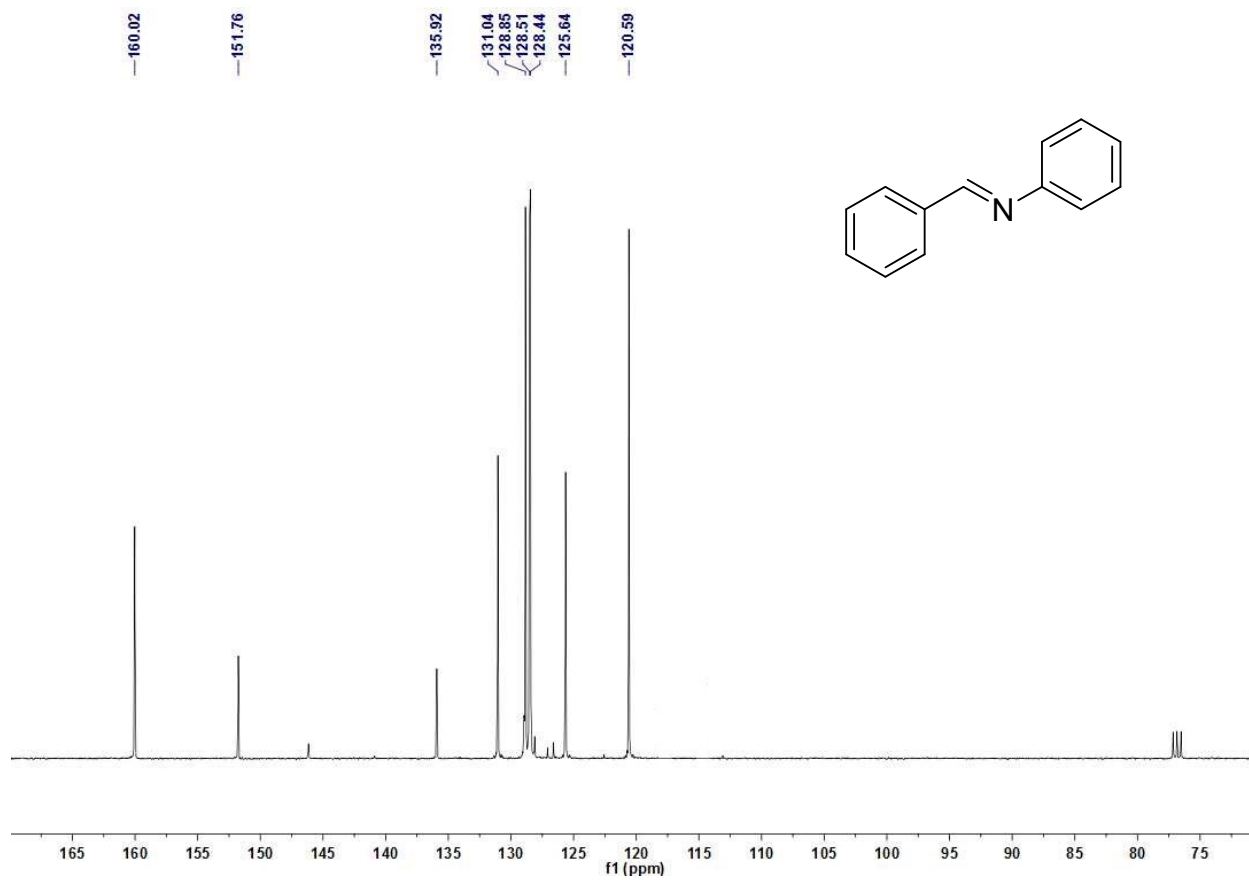


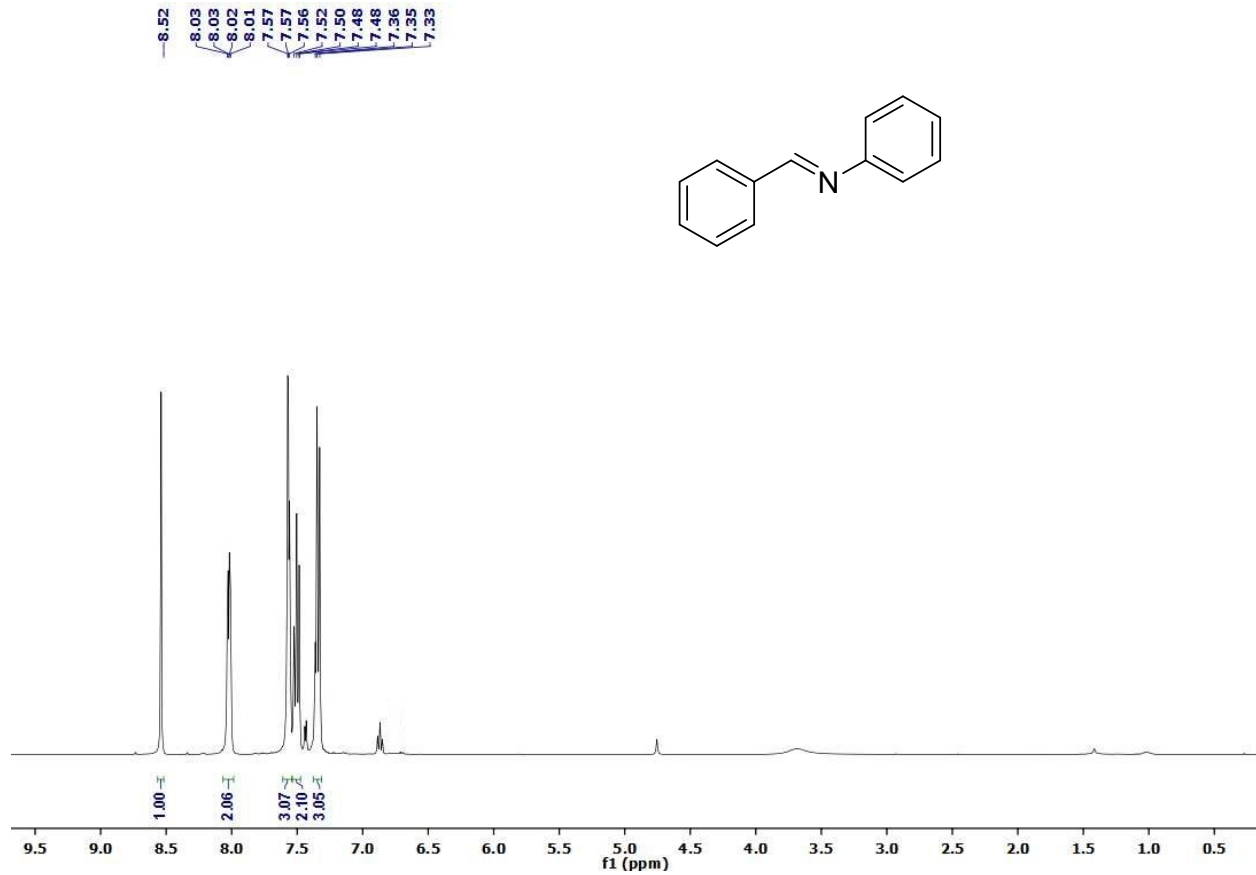


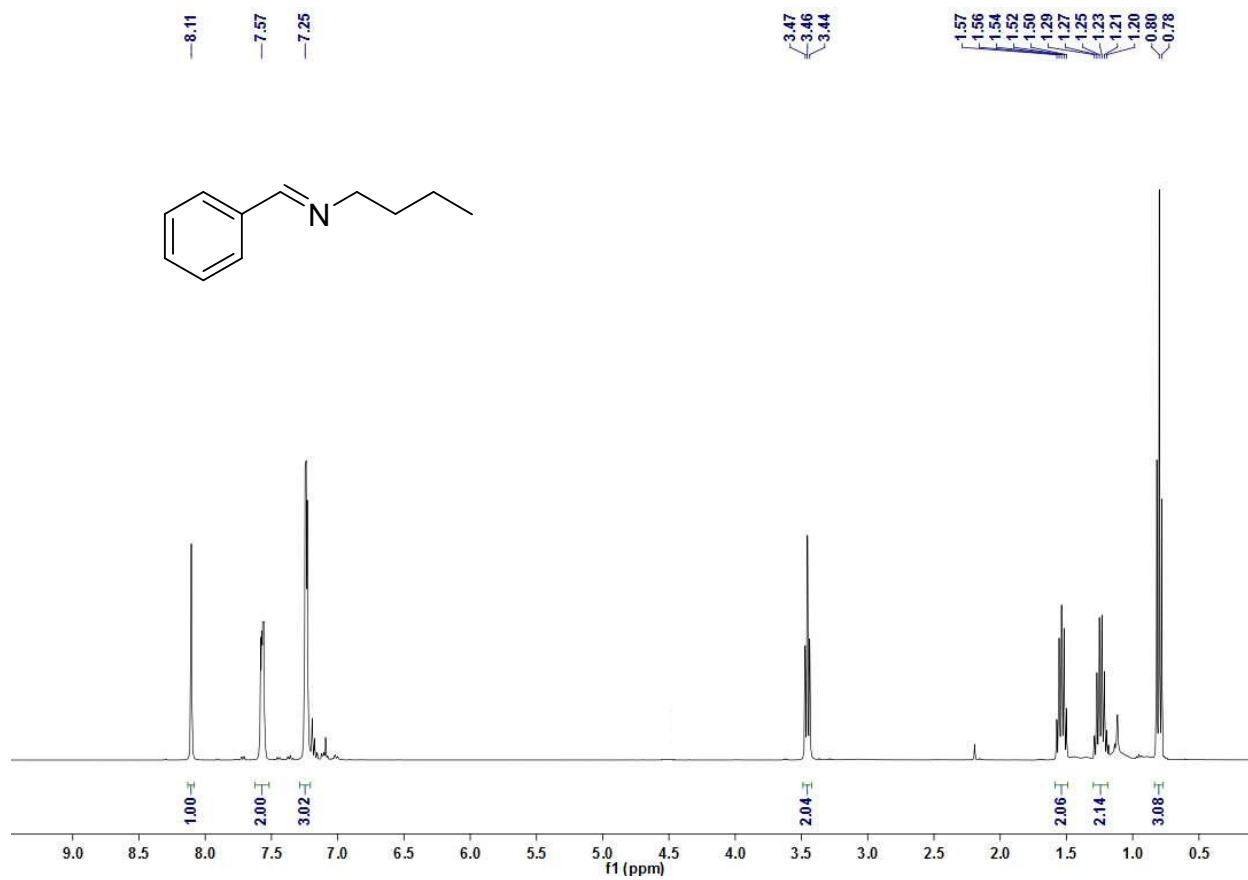


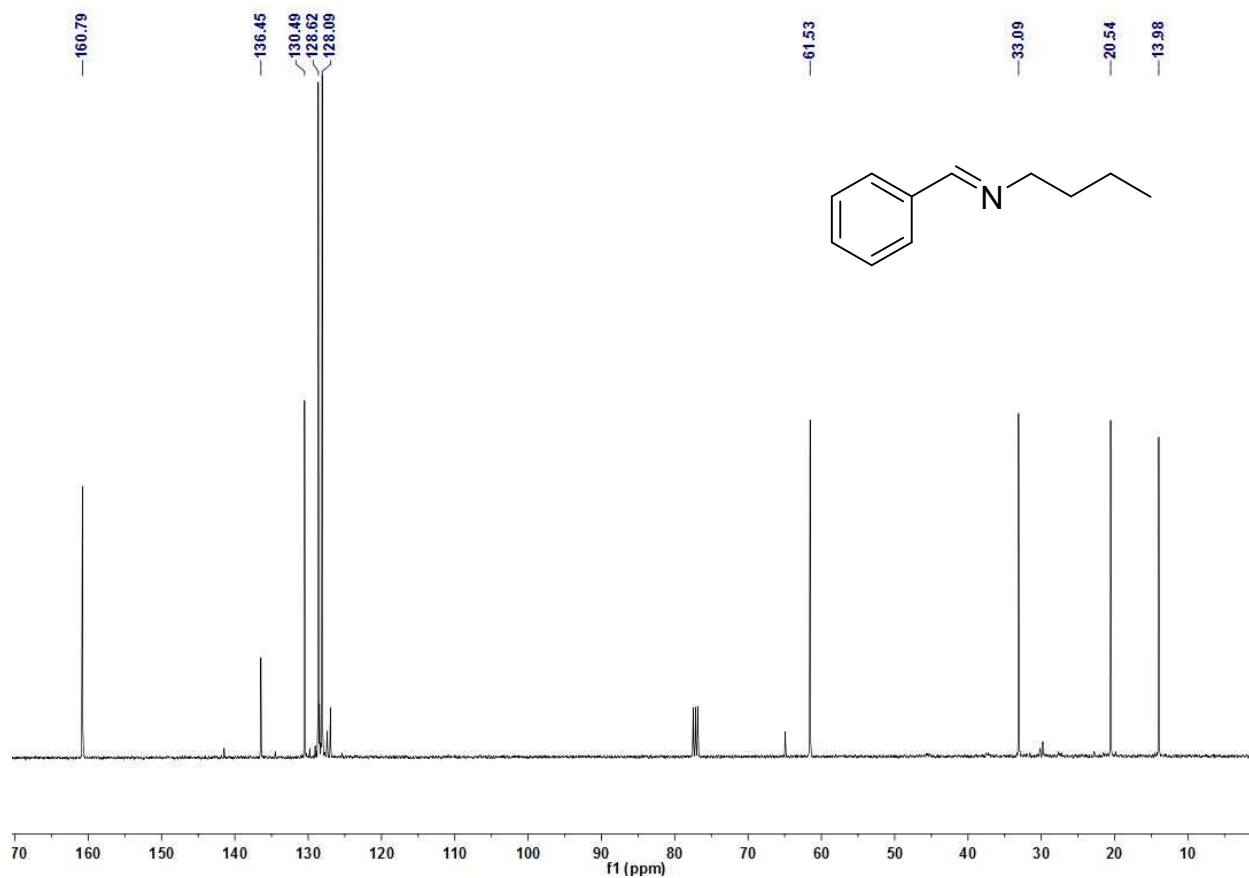












References:

- (1) Poyraz, A. S.; Song, W.; Kriz, D.; Kuo, C. H.; Seraji, M. S.; Suib, S. L. *ACS Appl. Mater. Interfaces* **2014**, *6* (14), 10986–10991.
- (2) NIST Chemistry WebBook <http://webbook.nist.gov/chemistry/> (accessed May 23, 2017).